

On the Stability of the Axially Compliant Fixed Scroll Member in Scroll Compressors

Hyun Jin Kim*

Key words: Scroll compressor, Axial compliance, Tipping moment, Sealing force

Abstract

Floating fixed scroll adopted for tip sealing enhancement in a scroll compressor is always under the influence of tipping moment produced by internal gas forces. Unless the tipping moment is properly compensated by some restoring moment, the fixed scroll would suffer tipping movement, degrading the compressor performance. The condition on which the tipping movement of the fixed scroll can be suppressed has been investigated analytically. For no tipping movement, the floating fixed scroll should be suspended on the main frame at proper level. The upper limit of the stable suspension is the axial location of the o-rings adopted for a back pressure chamber sealing on the rear side of the fixed scroll, and the lower limit is the mid-height of the scroll wrap.

| Nomenclature | | | |
|-----------------------------|---|-----------------------------|--|
| | | M_r, M_θ | : radial and tangential components of tipping moment |
| A | : area | M_t | : total tipping moment |
| c_1 | : constant | n | : number of suspension points for fixed scroll |
| F_a, F_{rg}, F_{tg} | : axial, radial, and tangential components of gas force | O_1, O_2 | : centers of fixed and orbiting scroll members |
| F_{seal} | : axial sealing force | P | : suspension location of fixed scroll |
| $F_{spx}, F_{spx}, F_{spz}$ | : components of spring force | Q | : contacting point between fixed and orbiting scroll members |
| f_s | : radial sealing force | r_a | : orbiting radius |
| h | : wrap height | $R_{cnx}, R_{cny}, R_{cnz}$ | : reaction components at contact point Q |
| k | : spring constant | V | : volume of compression chamber |
| l | : length | | |

* University of Incheon, Department of Mechanical Engineering, 177 Dowha-dong, Nam-gu, Incheon 402-749, Korea

Greek symbols

| | |
|------------|---|
| α | : tipping angle |
| β | : orientation angle of tipping moment |
| δ | : initial deflection of suspension means |
| η | : compressor efficiency |
| θ | : crank angle |
| θ_i | : circumference angle for suspension position |
| μ | : friction coefficient |

Subscripts

| | |
|-------|------------------------------|
| a | : axial direction |
| ad | : adiabatic |
| b | : back pressure chamber |
| c | : compression chamber |
| CB | : suspension point |
| cn | : contact point |
| d | : discharge |
| e | : discharge port |
| f | : fixed scroll |
| i | : i th leaf spring element |
| LS | : leaf spring |
| or | : o-ring |
| r | : radial direction |
| s | : suction or orbiting scroll |
| tip | : wrap tip |
| v | : volume |

1. Introduction

In general, the factors which affect the volumetric efficiency of refrigerating compressor are suction gas heating, clearance volume, wiring loss, and internal leakage, etc. One of the main advantages which scroll compressor has over other types of refrigerating compressors is its high volumetric efficiency. Scroll compressors have no clearance volume and no wiring loss at the valve passages. The suction gas heating, however, is the common problem

in degrading the volumetric efficiency, regardless of the type of the compressors of low side pressure. For hermetic type, the heat from the compressor motor is the main source of suction gas heating. For instance, the mass flow rate is known to be decreased by approximately 3~4% by suction gas heating in a typical 3 RT class compressor.

While internal leakage is minor for reciprocating type of compressors, it is the most critical form of gas leakage in scroll compressors. Two primary patterns of leakage between trapped compression pockets can occur: flank leakage through the radial clearance between the flanks of the two scroll wraps, and tip leakage through the axial clearance between scroll wrap tips and the mating scroll base plate. The latter can typically be several times the former.

In scroll compressors, various means of compliance mechanism for leakage control are widely used. Sliding bush is a typical means for radial compliance, and back pressure chamber mechanism is the most effective one for axial compliance. To achieve axial compliance, one of the two scroll members is allowed to move in the axial direction for limited range. A pressure chamber installed on the back side of the moving scroll member produces thrust on it against the other scroll member. Biasing pressure in the back pressure chamber may be provided from compression pockets via vents drilled in the base plate of the scroll member under compliance. When gas loading is applied on the fixed scroll member, it is usually suspended by means which are flexible axially, but very stiff in the other directions. One common design practice is to use leaf springs for suspending the fixed scroll member. A characteristic disadvantage of gas loading of axially compliant scroll member is a tipping moment, which is generated by gas pressure-induced forces inside compression pockets.⁽¹⁾ Balancing of tipping moment on the fixed

scroll member solely by over-pressurizing gas loading yields heavy tip load, leading to excessive frictional loss. Rather, reaction force at suspension of the fixed scroll member on the main frame can be effectively utilized to produce restoring moment.

In this study, the analysis has been carried on the stability of the axially compliant fixed scroll. The condition on which the fixed scroll can be free from tilting motion has been derived, and the effects of tilting of the fixed scroll member on the compressor efficiency have been estimated.

2. Stability analysis of fixed scroll

2.1 Axial sealing force

Fig. 1 shows a schematic view of axially compliant fixed scroll. Back pressure chamber is installed behind the fixed scroll. Gas of intermediate pressure is provided from compression pockets through vents on the base plate of the fixed scroll member. Downward gas loading is produced partly by discharge gas pressure and partly from back chamber pressure. As the crank shaft rotates, the orbiting scroll connected to the eccentric crank pin

orbits around the fixed scroll with the aid of anti-rotation device. Closely engaged two scroll members form inter-fitted crescent-shaped compression pockets and these pockets are moved inward, being reduced in size, as the crank shaft rotates. And eventually the compressed gas in the pockets is discharged into the discharge manifold through the discharge port at the center of the fixed scroll.

Since the orbiting scroll is axially supported by thrust bearing from behind, the axial movement of the orbiting scroll is limited within the oil film thickness of the thrust bearing. The fixed scroll, however, is supported by leaf springs at several peripheral locations around its rim so that its movement is only allowed in the axial direction for a limited range. This axial compliance suspension can alleviate the tight requirement for the axial clearance for tip sealing. Once the compressor starts to operate, the pressurized gas in the back chamber generates thrust large enough to overcome the axial gas force inside the compression pockets, pushing the fixed scroll against the orbiting scroll so that the tip sealing may be obtained.

Fig. 2(a)(b) show gas forces acting on the fixed scroll. F_a is the axial gas force which tends to move the two scrolls apart from each

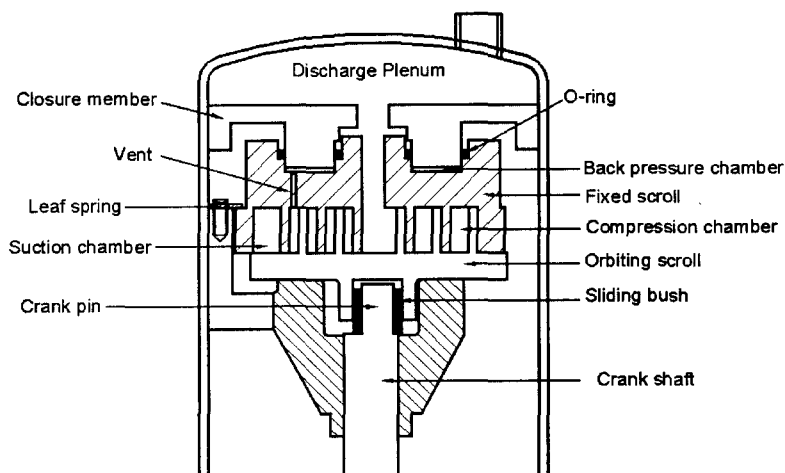


Fig. 1 Schematic diagram of scroll compressor.

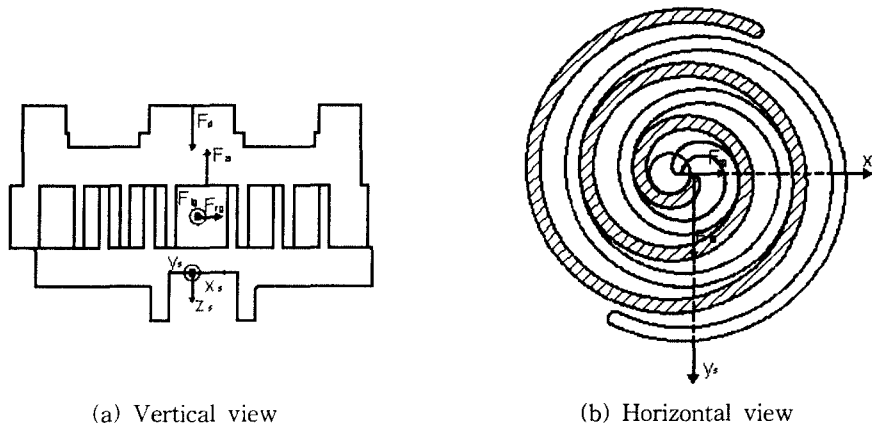


Fig. 2 Gas forces acting on fixed scroll member.

other, F_d is the thrust load from back, F_{rg} is the radial gas force which makes the two scrolls come closer in the radial direction, and F_{tg} is the tangential gas force acting on the orbiting scroll in the direction opposite to the orbiting motion, but on the fixed scroll in the same direction as the orbiting motion. As shown in Fig. 2(a), forces acting on the fixed scroll in the axial direction are the axial gas force F_a , thrust load F_d , and spring forces of leaf springs, $F_{spz,i}$ of Fig. 4. Resultant of these is the sealing force, F_{seal} , or the contacting force between the two scroll members as in the

equation (1).

$$F_{seal} = F_d - F_a - \sum F_{spz,i} \quad (1)$$

The spring forces are always upward since the fixed scroll is already lowered from its neutral position due to the net positive downward thrust force. Since, as shown in Fig. 3, operation envelope of refrigeration compressor is quite wide, it is not an easy task to keep optimum sealing force over the whole operating range. Optimum sealing force at higher discharge pressure conditions will become insufficient for tip sealing at lower discharge pressures, while optimum sealing force at lower discharge pressure conditions will cause excessive friction at higher discharge pressure conditions.

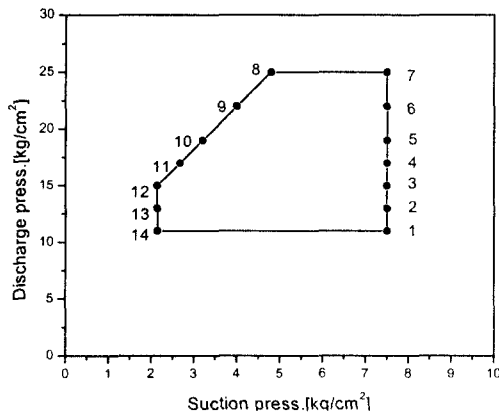


Fig. 3 Operating envelope for air conditioning compressor.

2.2 Tipping moment

Although the sealing force in the equation (1) is positive, there still exists a chance of gas leakage through the axial gap.

This possibility arises from tilting movement of the fixed scroll member induced by tipping moment. For the present model, the fixed scroll member is the floating one movable in the axial direction, and tipping moment is acting on the fixed scroll side. Fig. 4 illustrates the

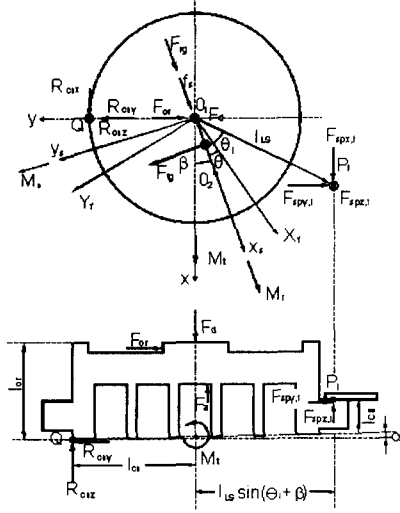


Fig. 4 Diagram of forces and moments acting on fixed scroll.

forces and moments exerting on the fixed scroll tilted by the tilting angle α in the counter clockwise direction due to tipping moment. O_1 is the center of the base circle of fixed scroll, and O_2 is that of the orbiting scroll. As the crank shaft rotates, the orbiting scroll center O_2 rotates around O_1 , and the coordinate system (x_s, y_s) rotates with O_2 by having x_s -axis always passing through O_2 , while coordinate system (X_f, Y_f) is fixed on the fixed scroll member. Axial gas force, F_a , and tangential gas force, F_{tg} , act on the mid-distance of $\overline{O_1O_2}$. Radial gas force, F_{rg} , and radial sealing force between scroll wrap flanks, f_s , act on the mid-height of the scroll wrap.

From Fig. 2 and Fig. 4, if we denote orbiting radius by r_a , and wrap height by h , the radial and tangential components of the tipping moment, M_r and M_θ , can be expressed by the equations (2) and (3), respectively.

$$M_r = F_{tg} \frac{h}{2} \quad (2)$$

$$M_\theta = F_a \frac{r_a}{2} - (f_s + F_{rg}) \frac{h}{2} \quad (3)$$

Resultant moment, M_t , and its orientation, β , measured from x_s -axis are expressed by the equations (4) and (5), respectively.

$$M_t = \sqrt{M_\theta^2 + M_r^2} \quad (4)$$

$$\beta = \tan^{-1}(M_\theta/M_r) \quad (5)$$

Here, another coordinate system (x, y) with its center at O_1 is defined by setting the x -axis being coincident with the orientation of resultant moment, M_t .

2.3 Suspension location for the fixed scroll

In order to find the condition for the fixed scroll to be free from the influence of tipping moment, the condition under which it becomes tilted will be first considered. As illustrated in Fig. 4, the fixed scroll member is assumed to be tilted by α in the counter clockwise direction under the influence of tipping moment. Since the tipping moment is always in the positive sense, the fixed scroll is never tilted in the clockwise direction.

Additional forces other than those presented in Fig. 2 are generated by the fixed scroll tilting. Inclination of the fixed scroll makes the two scroll members contact each other at Q , and the fixed scroll receives reaction force at the contacting point, Q , which lies on y -axis. R_{cx}, R_{cy} , and R_{cz} are the components of the reaction at Q in each direction. Also another reaction comes from the o-ring which is inserted at the top portion of the fixed scroll for the sealing of back pressure chamber as shown in Fig. 1. This reaction force, F_{or} , acts in $-y$ direction. Finally, reactions also arise at the spring connections. The point P_i represents

i th suspension point, and θ_i is the angular position of P_i measured from x_s -axis.

Then the balances of forces and moments exerted on the fixed scroll are given by the equations (6)~(8).

$$R_{cnz} - F_d + F_a + \sum_i F_{spz,i} = 0 \quad (6)$$

$$F_{or} + \sum_i F_{spy,i} - R_{cny} + (f_s + F_{rg}) \sin \beta - F_{ig} \cos \beta = 0 \quad (7)$$

$$M_t - l_{cn}(F_d - F_a) - F_{or} l_{or} - l_{CB} \sum_i F_{spy,i} + \sum_i F_{spz,i} \{l_{cn} + l_{LS} \sin(\theta_i + \beta)\} = 0 \quad (8)$$

Here, l_{CB} and l_{or} are the axial distances from the fixed scroll wrap tip to the leaf springs and the o-ring, respectively. For small tilting angle α , the reaction from the o-ring, F_{or} , and the spring force in the axial direction, $\sum F_{spz,i}$, can be expressed by the equations (9) and (10), respectively.

$$F_{or} = \alpha k_{or} l_{or} \quad (9)$$

$$\sum F_{spz,i} = \sum k \{ \delta - \alpha (l_{cn} + l_{LS} \sin(\theta_i + \beta)) \} \quad (10)$$

Here, δ is the spring displacement in the axial direction, that is, the displacement of the fixed scroll from its neutral position due to the thrust, F_d .

If the friction coefficient at the contacting point Q is denoted by μ , y -component of the reaction force, R_{cny} , can be set to $R_{cny} = \mu R_{cnz}$. From the equations (6) and (7),

$$\sum_i F_{spy,i} = F_{ig} \cos \beta - (f_s + F_{rg}) \sin \beta - F_{or} + \mu (F_d - F_a - \sum_i F_{spz,i}) \quad (11)$$

Substituting the equation (11) together with the equations (9) and (10) into the equation (8), the moment balance on the fixed scroll can be rewritten by the equation (12).

$$\begin{aligned} & M_t - l_{cn}(F_d - F_a) - \alpha k_{or} l_{or}^2 \\ & + k \sum \{ [\delta - \alpha (l_{cn} + l_{LS} \sin(\theta_i + \beta))] \\ & \times (l_{cn} + l_{LS} \sin(\theta_i + \beta)) \} \\ & - l_{CB} [F_{ig} \cos \beta - (f_s + F_{rg}) \sin \beta] \\ & - \alpha k_{or} l_{or} + \mu (F_d - F_a) \\ & - \mu k \sum \{ \delta - \alpha (l_{cn} + l_{LS} \sin(\theta_i + \beta)) \} = 0 \end{aligned} \quad (12)$$

This can also be rearranged for the tilting angle α as follows.

$$\alpha = \frac{[M_t - l_{cn}(F_d - F_a) + k(l_{cn} \sum \delta + \delta l_{LS} \sum \sin(\theta_i + \beta)) - l_{CB}(F_{ig} \cos \beta - (f_s + F_{rg}) \sin \beta + \mu(F_d - F_a) - \mu k \sum \delta)]}{[k_{or} l_{or}^2 + 2kl_{SL}(l_{cn} \sum \sin(\theta_i + \beta) + kl_{LS}^2 \sum \sin^2(\theta_i + \beta)) + nk_{cn} l_{cn}^2 - k_{or} l_{or} l_{CB} + \mu kl_{CB} \sum \{l_{cn} + l_{LS} \sin(\theta_i + \beta)\}]} \quad (13)$$

Since for equally distanced leaf springs, $\sum \sin(\theta_i + \beta) = 0$ and $\sum \sin^2(\theta_i + \beta) = c_1$ (c_1 is constant), the tilting angle α can be expressed by the equation (14).

$$\alpha = \frac{[M_t - l_{cn}(F_d - F_a) + kl_{cn} \sum \delta - l_{CB}(F_{ig} \cos \beta - (f_s + F_{rg}) \sin \beta + \mu(F_d - F_a) - \mu k \sum \delta)]}{[k_{or} l_{or} (l_{or} - l_{CB}) + k(c_1 l_{LS}^2 + n l_{cn}^2 + \mu n l_{CB} l_{cn})]} \quad (14)$$

To find the condition of $\alpha > 0$, that is, the condition that the fixed scroll becomes tilted, both of the denominator and the numerator of the equation (14) should be simultaneously positive or negative. The conditions for both of the denominator and numerator to be positive are as in the equations (15) and (16), respectively.

$$l_{CB} < l_{or} \frac{1 + \left(\frac{k}{k_{or}}\right) \left\{ c_1 \left(\frac{l_{LS}}{l_{or}}\right)^2 + n \left(\frac{l_{cn}}{l_{or}}\right)^2 \right\}}{1 - \mu n \left(\frac{k}{k_{or}}\right) \left(\frac{l_{cn}}{l_{or}}\right)} \quad (15)$$

$$l_{CB} < \frac{M_t - l_{cn}(F_d - F_a) + kl_{cn}\sum\delta}{[F_{tg}\cos\beta - (f_s + F_{rg})\sin\beta + \mu(F_d - F_a) - k\mu\sum\delta]} \quad (16)$$

After some manipulation, the equation (16) can be rewritten by the equation (17).

$$l_{CB} < \frac{\frac{h}{2\cos^2\beta} - l_{cn}\frac{F_{seal}}{F_{tg}\cos\beta}}{1 - \frac{f_s + F_{rg}}{F_{tg}}\tan\beta + \mu\frac{F_{seal}}{F_{tg}\cos\beta}} \quad (17)$$

And the conditions for both of the denominator and numerator to be negative are as in the equations (18) and (19), respectively.

$$l_{CB} > l_{or} \frac{1 + \left(\frac{k}{k_{or}}\right)\left\{c_1\left(\frac{l_{LS}}{l_{or}}\right)^2 + n\left(\frac{l_{cn}}{l_{or}}\right)^2\right\}}{1 - \mu n\left(\frac{k}{k_{or}}\right)\left(\frac{l_{cn}}{l_{or}}\right)} \quad (18)$$

$$l_{CB} > \frac{\frac{h}{2\cos^2\beta} - l_{cn}\frac{F_{seal}}{F_{tg}\cos\beta}}{1 - \frac{f_s + F_{rg}}{F_{tg}}\tan\beta + \mu\frac{F_{seal}}{F_{tg}\cos\beta}} \quad (19)$$

Therefore, the condition that the fixed scroll becomes unstable, being tilted due to the tipping moment, turns out to be the range of l_{CB} which falls in the common area indicated by the equations (15) and (17), or in that by the equations (18) and (19). Since the range of l_{CB} indicated by the equation (17) is included in that of the equation (15), the common area of these two ranges is the range of the equation (17). Also the common area of the two ranges of the equations (18) and (19) is the range of the equation (18). Therefore, it can be stated that the fixed scroll becomes unstable when it is suspended by the suspension means such as leaf springs at the axial position of l_{CB} which lies in the range indicated by the equation (17) or the equation (19). The range outside the ranges indicated by the equations (17) or (19) can be written by the equation (20).

$$l_{or} \frac{1 + \left(\frac{k}{k_{or}}\right)\left\{c_1\left(\frac{l_{LS}}{l_{or}}\right)^2 + n\left(\frac{l_{cn}}{l_{or}}\right)^2\right\}}{1 - \mu n\left(\frac{k}{k_{or}}\right)\left(\frac{l_{cn}}{l_{or}}\right)} > \frac{\frac{h}{2\cos^2\beta} - l_{cn}\frac{F_{seal}}{F_{tg}\cos\beta}}{1 - \frac{f_s + F_{rg}}{F_{tg}}\tan\beta + \mu\frac{F_{seal}}{F_{tg}\cos\beta}} \quad (20)$$

Therefore, it can be stated that if the fixed scroll is suspended to the main frame by means of suspension such as leaf springs within the axial location indicated by the equation (20), the fixed scroll can be made free from tilting, in spite of the presence of tipping moment.

Since l_{or} , l_{cn} , and l_{LS} are about the same order of magnitude, but the stiffness of the o-ring is much greater than that of leaf springs, that is, $k_{or} \gg k$, the upper limit of l_{CB} of the equation (20) can be rewritten as follows.

$$l_{or} \frac{1 + \left(\frac{k}{k_{or}}\right)\left\{c_1\left(\frac{l_{LS}}{l_{or}}\right)^2 + n\left(\frac{l_{cn}}{l_{or}}\right)^2\right\}}{1 - \mu n\left(\frac{k}{k_{or}}\right)\left(\frac{l_{cn}}{l_{or}}\right)} \simeq l_{or} \quad (21)$$

Then, the condition of stable suspension for the fixed scroll can be expressed by the equation (22).

$$l_{or} > l_{CB} > \frac{\frac{h}{2\cos^2\beta} - l_{cn}\frac{F_{seal}}{F_{tg}\cos\beta}}{1 - \frac{f_s + F_{rg}}{F_{tg}}\tan\beta + \mu\frac{F_{seal}}{F_{tg}\cos\beta}} \quad (22)$$

3. Calculation results and discussions

3.1 Sealing force and tipping moment

The stability analysis of the floating fixed scroll member discussed so far has been applied to a 3 hp-class scroll compressor using refrigerant R-22. The radius of the basic circle of the scroll wrap configuration is 2.04 mm, the wrap end angle is 1205°, wrap height is 25 mm,

and the wrap thickness is 2.55 mm. The gas pressure in the compression pockets is calculated from adiabatic compression assumption, and the gas forces are calculated from the gas pressure in the compression pockets. The details of these calculation methods can be referred to the open literature.^(2,3,5)

Fig. 5 shows various forces acting on the fixed scroll at ARI condition. Variation of the tip sealing force, F_{seal} , with the crank angle is related to the variation of F_a . Radial gas force, F_{rg} is considerably small compared to other gas forces, and the radial sealing force between the scroll wrap flanks, f_s is greater than

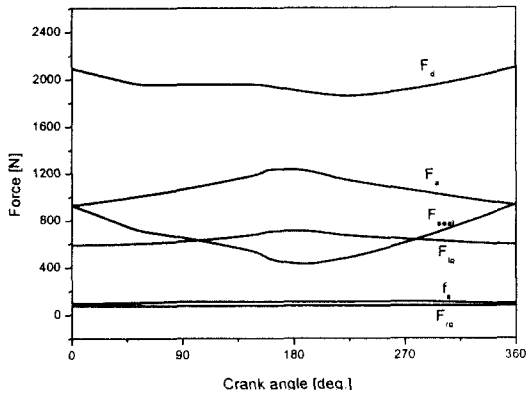


Fig. 5 Various forces acting on fixed scroll at ARI condition.

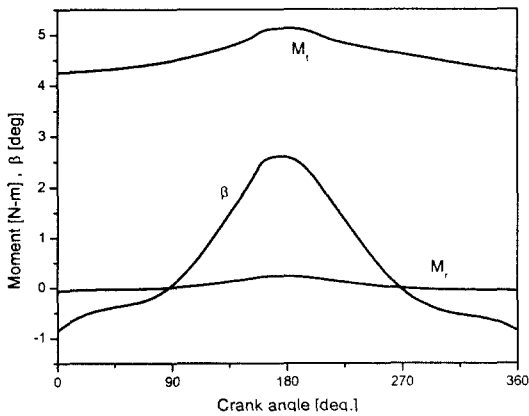


Fig. 6 Overturning moments and direction angle.

F_{rg} by centrifugal force of the orbiting scroll. The tipping moment and its orientation are shown in Fig. 6. Tangential component of the tipping moment, M_θ , is so small compared to radial component, M_r , that $M_\theta \cong M_t$ and $\beta < 4^\circ$. This implies that the orientation of the tipping moment can be practically regarded to nearly coincide with x_s -axis.

3.2 Suspension position

The forces involved in the equation (22) change with operation condition as well as

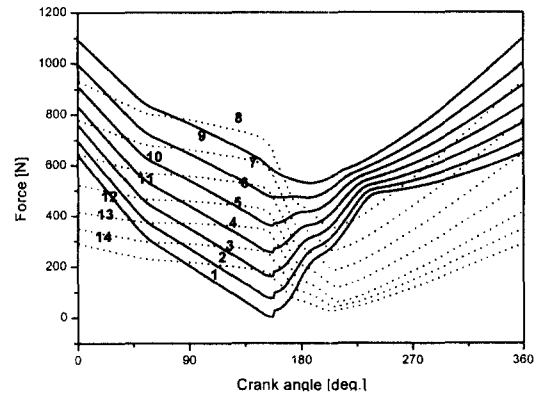


Fig. 7 Axial sealing force at various operating conditions.

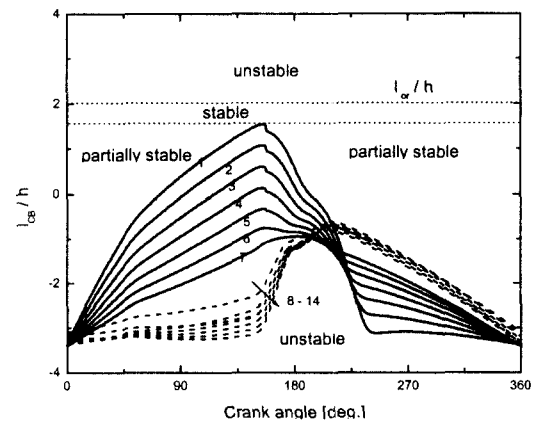


Fig. 8 Stable suspension range for no tipping motion of the fixed scroll.

with the crank angle. The variations of F_{seal} are shown in Fig. 7. Numbers in Fig. 7 indicate the operation conditions of Fig. 3. Fig. 8 shows the range of l_{CB} for stable fixed scroll compliance at various operation conditions. The lower limit of l_{CB} varies with the crank angle and the operation condition as well, while the upper limit of l_{CB} is fixed at the axial location of the o-rings as indicated in the equation (22). The most restrictive condition comes from the operation condition #1, which determines the lower limit of l_{CB} effective over all the operation conditions suggested in Fig. 3. If the fixed scroll is suspended at l_{CB} belonging to the range indicated as 'partially stable' of Fig. 8, it would suffer tilting for the duration of time when the crank shaft is passing the angular zone indicated as 'unstable'.

In fact, once the compressor's main design specifications are given, the gas forces and tipping moment are subsequently determined, and these magnitudes can not be changed at one's option. Hence, in order to widen the range of l_{CB} , the only remaining parameter is the tip sealing force, F_{seal} . The tip sealing force can be easily controlled by changing acting area of the back pressure chamber.

The lower limit of l_{CB} can not rise above $h/2$. Because β and μ are small enough and F_{tg} is larger than f_s and F_{rg} , the numerator of the equation (22) approaches to $h/2 - l_{cn} \cdot F_{seal}/F_{tg}$, which is of course smaller than $h/2$, while the denominator approaches to 1. Hence, the fixed scroll can be made safe from any tilting motion for $l_{or} \geq l_{CB} \geq h/2$ regardless of the operation condition, as long as the tip sealing force is greater than zero.

Caillat et al.⁽⁴⁾ and Bush and Elson⁽¹⁾ argued that any tipping moment in the fixed scroll could be avoided by placing mounting means at the level of the center of the vanes, that is,

$l_{CB} = h/2$, so that the mechanical reaction is essentially in line with F_{tg} , which is mainly responsible for generation of the tipping moment. According to Fig. 8, however, it has been demonstrated that full balancing of any significant tipping movement of the fixed scroll can be achieved as far as it is mounted in the range of $l_{or} \geq l_{CB} \geq h/2$.

3.3 Effects of tilting on compressor efficiency

In case of mounting the fixed scroll in the 'partially stable' range of Fig. 8, the fixed scroll suffers tipping movement over some crank angles in one cycle. This would augment gas leakage through enlarged leak passage and decrease the compressor efficiency. Compressor performance has been calculated at several tilting angles by using computer simulation program.⁽⁵⁾ Fig. 9 shows the effects of tipping movement on the volumetric efficiency and gas compression efficiency at ARI condition. The efficiencies are normalized by those at no tipping movement. As the tilting angle α increases, both of the volumetric and gas compression efficiencies decrease rapidly. The maximum tip opening between the two scroll members at the tilting angle of $\alpha = 0.03^\circ$ corresponds to $36 \mu\text{m}$. At this much tilting, and the volu-

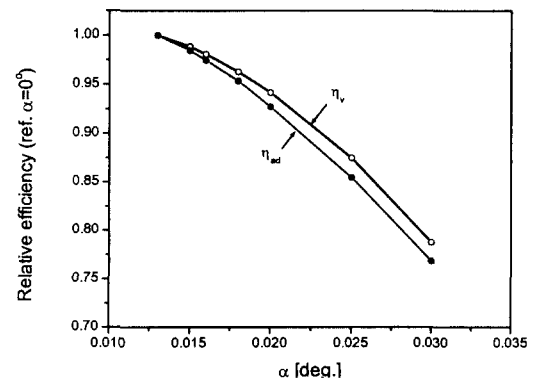


Fig. 9 Effect of fixed scroll tilting on volumetric and adiabatic efficiencies.

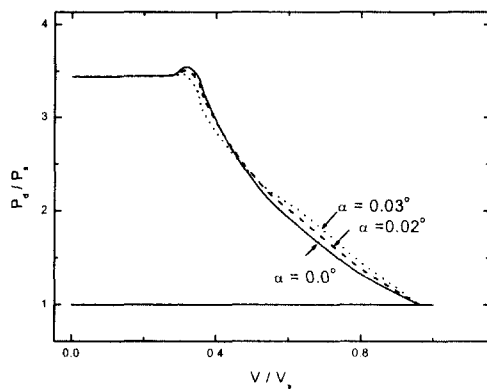


Fig. 10 Effect of fixed scroll tilting on p-v diagram.

metric and the compression efficiencies drop by 23.9% and 27.1%, respectively. For the tilting of $\alpha < 0.013^\circ$, the efficiencies are not affected by the scroll tilting, since the opening induced by fixed scroll tilting is about the same size as the oil film thickness in the axial gap between the two scroll members.

P-V diagrams at three different tilting angles are compared at Fig. 10. At larger tilting angle, the pressure becomes higher in the first half of the compression process, but lower in the second half. This is because more gas leakage from high pressure pockets to low pressure pockets is incurred at larger tilting angle.

4. Conclusions

For scroll compressor which has a back pressure chamber behind the fixed scroll so that it may be made movable in the axial direction for axial compliance to improve tip leakage control, an analytical study has been carried on the stability of the fixed scroll and the following conclusions have been obtained.

(1) The range of the suspension position of the fixed scroll on the main frame in order that the fixed scroll may be free from any

tipping movement despite of the influence of tipping moment has been analytically found as in the equation (22).

(2) Full balance of any significant tipping movement of the fixed scroll can be achieved, as far as it is mounted in the range of $l_{or} \geq l_{CB} \geq h/2$, that is, the level between the o-ring location and the scroll wrap mid-height.

(3) Even small tipping movement of the fixed scroll has been found to yield severe degradation of the compressor efficiency. The compressor performance is decreased by as much as 25% at the tilting angle of $\alpha = 0.03^\circ$.

References

1. Bush, J.W. and Elson, J.P., 1990, Scroll compressor design criteria for residential air conditioning and heat pump applications, Part I: Mechanics Proceedings of International Compressor Engineering Conference at Purdue, pp. 83-92.
2. Morishita, E., Sugihara, M., Inaba, T., Nakamura, T. and Works, W., 1984, Scroll Compressor Analytical Model, Proceedings of International Compressor Engineering Conference at Purdue, pp. 487-495.
3. Tojo, K., Ikegawa, M., Maeda, N., Machida, S. and Shiibayashi, M., 1986, Computer modeling of scroll compressor with self adjusting back pressure mechanism, pp. 872-886.
4. Caillat, J.M., Weatherston, R.C. and Bush, J.W., 1988, Scroll type machine with axially compliant mounting, U.S. Patent No. 4,767,293.
5. Kim, H.J., Kim, J.H. and Lee, J.K., 1998, Dynamic behavior of a scroll compressor with radial compliance device, Korean Journal of Air-Conditioning and Refrigeration Engineering, Vol. 10, No. 1, pp. 33-43.